Adsorption and Desorption of Sulfur Compounds by Improved Nano Adsorbent: Optimization Using Response Surface Methodology

Bakhtiari, Ghasem
Chemistry Departments, Amirkabir University of Technology, P.O. Box 15875-4413, Tehran, I.R. IRAN

Bazmi, Mansour*[+]
Refining Technology Development Division, Research Institute of Petroleum Industry, Tehran, I.R. IRAN

Abdouss, Majid*[+]
Chemistry Departments, Amirkabir University of Technology, P.O. Box 15875-4413, Tehran, I.R. IRAN

Royaee, Sayed Javid
Refining Technology Development Division, Research Institute of Petroleum Industry, Tehran, I.R. IRAN

ABSTRACT: *Today, sulfur removal from fuels has improved by new adsorbents such as zeolites that needs extensive studies. This study investigates the feasibility of sulfur compounds adsorption on improved nano zeolite existing in organic fuels and desorption of them from nano-adsorbent. Some properties of improved nano zeolite were analyzed to receive better sulfur compounds adsorption. Zeolite surface structure was analyzed by TEM (tunneling electron microscopy). Batch experiments were chosen for adsorption/desorption study of sulfur compounds and adsorption and desorption conditions were optimized by BBD methodology. The influence of variables in the process, consists of adsorbent metal percent (0.05-10* wt%*), adsorbent calcination temperature (200-500 °C) and adsorption process temperature (30-120 °C) in adsorption stage and gas flow rate (1.5-3.5 mL/Min), regeneration temperature (150-300 °C) and desorption time (30-90 Min) which were investigated using experimental design procedure.*

KEYWORDS: *RSM; Nano zeolite; Adsorption; Regeneration.*

INTRODUCTION

Adsorbents capture in adsorption processes has been carried out by many researches in recent years. Some researchers have studied extensively to present suitable adsorbents. X-zeolite and Y-zeolite show some promising potentials in adsorption technology applications [1-4]. These zeolites have high potential in adsorption of sulfur and nitrate compounds. Adsorption condition for sulfur and nitrogen compounds on nano X-zeolites and nano Y-zeolites have not been investigated by researchers. Analysis of adsorption characteristics for sulfur compounds

***** *To whom correspondence should be addressed.*
+ E-mail: bazmim@ripi.ir ; phdabdouss44@aut.ac.ir
1021-9986/2017/4/69-79 11/$/6.10

permeation factors is important based on selectivity factors. Also, prediction of adsorption and desorption behavior in the adsorption system needs to be studied. [5-10]

The optimum point of the adsorption process is of great importance for all developed processes. Process dynamics and process characteristics are required for modeling and optimization of the process. The adsorption and its dynamic characteristics are complicated phenomena; some efforts have been made to develop experimental design procedure and optimization of a methodology that can help researchers to further complete the experimental design procedures such as some effects of independent variables on dependent variables. [11-14]

Adsorption processes are usually optimized with RSM (Response Surface Methodology). Efficiency of sulfur removal by an adsorption process depends on adsorbent metal dose, initial sulfur concentration, process temperature and adsorption time. Initial sulfur concentration of feed depends on actual feed sources or model feed. As initial sulfur concentration of feed is related to considered industry and its products, this parameter cannot be optimized in these studies. Therefore, adsorption and desorption processes have been optimized with adsorbent metal dose, process temperature and adsorption time (independent process parameters). Sulfur compounds in fuels are harmful for humans and environment. Sulfur compounds need proper treatment before using as fuels components in engines. Many chemical and physical methods including, membrane, precipitation, adsorption, ODS (Oxidative desulfurization) and HDS (Hydrodesulfurization) have been used for desulfurization of hydrocarbon effluents [15-18]. Adsorption method is one of the best methods for motor fuel treatment, although regeneration of saturated sulfur adsorbents is the main disadvantage of sulfur adsorption process. Improved zeolites can be used as sulfur adsorbent to reduce environmental pollution of fuels [19,20]. Previous studies show that recycling and regeneration of saturated sulfur adsorbents is possible without any problems in formation of sludge. Studies show that sulfur adsorption by improved zeolites depends on metal percentage on support, process time and the adsorption temperature [21]. Through the researches carried out, finding the optimum adsorption condition (metal percent, process time, adsorption temperature) for sulfur removal is essential to get the most and the best sulfur removal efficiency. Studies demonstrated that sulfur adsorption from fuels can be optimized by Response Surface Methodology (RSM). A lot of researches have proved that Response Surface Methodology (RSM) is an essential statistical tool for optimization of sulfur removal and adsorption processes [22-25]. Response Surface Methodology (RSM) is a mathematical technique and collection of statistics is useful for optimizing, improving, and developing processes [26]. First, this methodology was described and developed by *Wilson and Box* [27]. Response Surface Methodology (RSM) is so useful, economical and a practical tool for analysis of processes and its modeling by polynomials to the true output and input relationship as local approximations [28-31]. RSM (Response Surface Methodology) has several advantages compared to the classical methods. Classical optimization methods involve changing a variable at one time that is quite time consuming especially when a lot of variables are to be considered. [32]

In the present paper, we focus on decreasing sulfur compounds, optimization of adsorption conditions and investigation of effect of parameters on sulfur compounds influence to achieve to the best performance. AgX zeolite as an adsorbent was prepared by impregnating Ag on X-zeolite [21].

EXPERIMENTAL SECTION

Materials

All chemicals and solvents were analytical grade and directly used as received without any further purification. Anhydrous sodium aluminate, sodium hydroxide pellets 99%, aqueous colloidal silica 30 wt.% SiO_2 (HS-30) were used from Aldrich.

thiophene (98 wt%), $AgNO_3$(99.9 wt%) and iso-octane (99 wt%) were purchased from Merck.

Chemical and Physical Analysis.

TEM (Transmission Electron Microscopy) was carried out on the device model of CM-200 from Philips Company. Sample for TEM measurement was dispersed by ultrasonic bath in ethanol. Moreover, a FFT (Fast Fourier Transformation) was performed to examine closely the flow-induced orientational patterns.

For Gas Chromatography (GC) Analysis, the sample collected during the breakthrough experiment was analyzed using a Agilent 7890 with a flame photometric detector

and an EC-5 capillary column (L) 50 m; (i.d.) 0.32 mm. The column final temperature values were 240 °C for thiophene analysis. The column temperature program was set to increase from 70 °C to a set value at a 2 °C/min rate. Retention time for thiophene was 7.1 min (thiophene diluted in sulfur-free n-octane to a known concentration) and the injector temperature was set to 200 °C.

The total test time for thiophene component in the GC column was above 9.5 min. The signals (peaks) are similar to those found in the literature for similar analysis setup and conditions. To establish the detection limit of the GC-FPD, solutions of thiophene in n-octane, prepared by sequential dilution, were used. Detectable peaks were recorded at concentrations down to 0.148 ppm thiophene or 0.56 ppm sulfur. The peak was no longer visible for the 0.18 ppm sulfur solution. The intensity was comparable with noise level. Thus, the minimum detection was about 0.56 ppm sulfur.

Nitrogen isotherm was measured with an ASAP 2020 (Micromeritics) at 77 K. The sample was heated to a constant pressure, under a vacuum of 10-2 Pa, at 305 °C and out gassed overnight at this temperature, before experiment. The isotherms could be used to calculate the micropore volume (V_{mic}), specific surface area (S), average micropore size (L_{mic}), pore size distribution (*DFT*) and total pore volume (V_t).

X-Ray Diffraction (XRD) pattern was recorded a Bruker D8 Advance diffractometer with a Cu KR monochromatized radiation source, operated at 30 mA and 40 kV with a scan speed of 0.05°/0.2 s.

FT-IR (Fourier Transform-Infra Red) tests were done with Vertex-70 (Bruker factory) that had a combine reactor and small cell.

Synthesis and improvement of sorbents

According to the study in the previous literature [21], Synthesized 13X-zeolite with the molar ratio of $3.4Na_2O:Al_2O_3: 2.9SiO_2:150H_2O$ was prepared by adding aqueous colloidal silica to aqueous sodium aluminate. After stirring at ambient temperature for 45 min and then 22 h and 108 °C ageing in Teflon autoclave, completed reactions. Solid products washed and dried at 100 °C.

Adsorption/ Desorption Study

Adsorption/ Desorption experiments were performed by a batch method. For Adsorption a model feed consisting of *iso*-octane of 3.5 mmol (432 ppm as Sulfur) and thiophene was used as an organic solution. The 0.5 g from improved adsorbent and the 10 mL from model feed, mixed into a stainless steel tube with 50 mL volume and shaking for 4 h with desired temperatures. The produced liquid was separated from the saturated adsorbent and the thiophene concentration in the product was analyzed by an Agilent GC 7890 sulfur analyzer. The sulfur determination error in experimental tests was +0.56,-0.56 ppm.

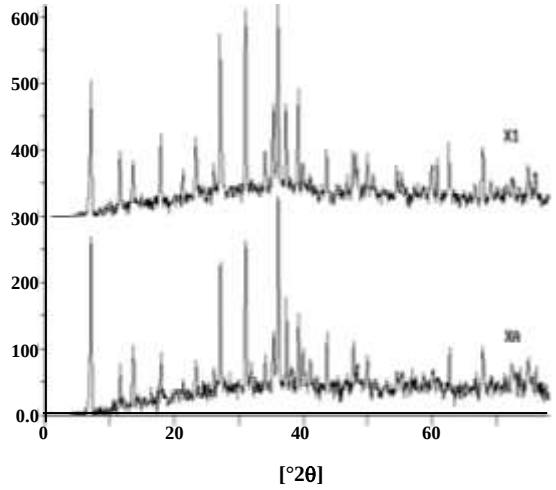

Fig. 1: XRD patterns of (XA) fresh AgX-zeolite and (X1) regenerated AgX-zeolite.

Desorption of sulfur compounds from improved adsorbent was tested with heat gas flow. XRD patterns of Fresh and regenerated sorbent shown in Fig. 1. After appropriate evacuation sulfur compounds and hydrocarbons from adsorbents and cooling step, the breakthrough tests again was down. The adsorption–desorption process was taken several times with model feed. Desorption process was taken in 234 and 2.4 mL/min air flow for 72 min. For checking the adsorbent surface after desorption, the adsorbents were investigated via TEM. Fig. 2(a),(b) illustrated the TEM images of regenerated and fresh adsorbent after several time regeneration. Figures show nano structure stability of adsorbents in both sections.

Experimental design

The Experimental design was used for the maximization of sulfur adsorption on nano AgX-zeolite and their regeneration. The BBD (Box-Behnken) method was chosen for investigation of factors effects on the desorption process: desorption time, gas flow, desorption

Table 1: Experimental ranges and levels in the experimental design.

Factor	A		B		C	
Process	Adsorption Temp. (°C)	Desorption Temp. (°C)	Adsorbent Metal wt%	Gas Flow Desorption (mL/min)	Adsorbent Temp. Calcination(°C)	Desorption Time (min)
Range and Level	30	150	0.5	0.5	200	30
	75	225	5.25	2	350	60
	120	300	10	3.5	500	90

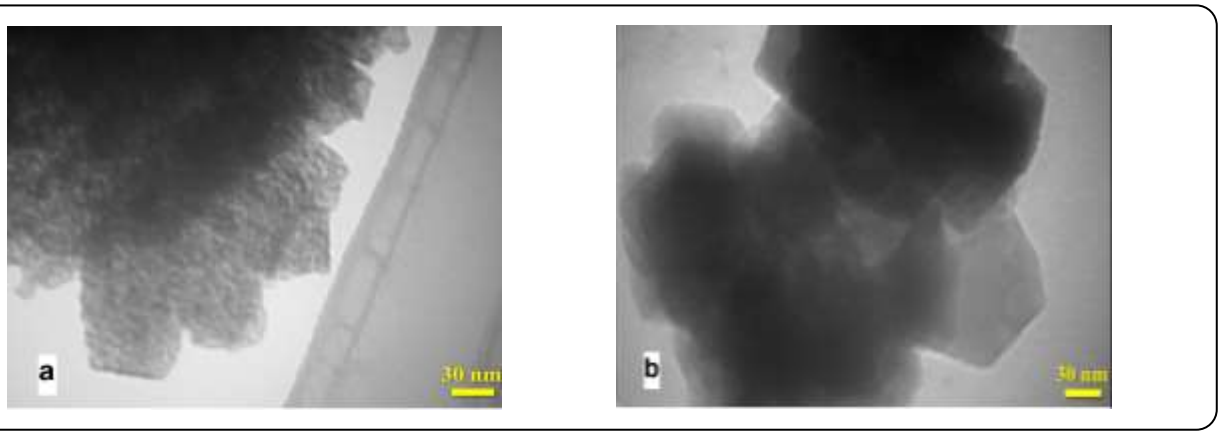

Fig. 2: TEM images of (a) fresh nano AgX-zeolite.(b) regenerated nano AgX-zeolite.

temperature: and sorption process: metal percent (wt%), calcinations temperatures (°C), adsorption temperatures (°C) as shown in Table 1. The 2K factorial design only requires three levels of each factor and is rotatable. Each factor was studied at three different levels (±1, 0). The inclusion of centre points offered a more precise estimate of provided a measure for the adequacy of the model (lack of fit) and experimental error. It also enabled the determination of the significance of the interactions between factors. The correspondence between the coded and real forms and the level of the investigated factors are listed in Table 2.

RESULTS AND DISCOSSION

Characterization of fresh and regenerated adsorbent

The XRD patterns of the AgX-zeolite and regenerated adsorbent at 245 °C are noticed in Fig. 1 Both fresh impregnated adsorbent and regenerated adsorbent were dark color. The similarity in the XRD patterns and lattice parameter values of AgX-zeolite and regenerated adsorbent (Table 3) indicates that the both sorbent structure (AgX-zeolite and regenerated zeolite) was retained after process followed after heat stages consist of calcinations for fresh adsorbent and hot gas flow for desorption process. Although oxidation reactions of SO_2 gas production (sulfur compounds burning) in desorption process and the impregnated metal ions take place for fresh adsorbents during the heating. The components of the fresh AgX-zeolite and the regenerated adsorbents are summarized in Table 3.

The results analyses noticed that the processes of calcination, impregnate and regenerating by gas flow did not have any significant effects in adsorbents.

The FT-IR spectra (Fig. 3) of the sulfur compounds (thiophene) saturated adsorbent and regenerated adsorbent corresponded to the fresh sorbent (13X-zeolite). Main peaks skeletal vibration: in 749, 667 cm^{-1}; 976 cm^{-1}tetrahedron stretching vibration peak with a shoulder at 1055 cm^{-1}, regenerated zeolite has the main characteristic of peak at 617 cm^{-1}, T–O bending vibration peak of 459 cm^{-1}, double 6 ring vibration peak of 563 cm^{-1} and a peak at 3465 cm^{-1} indicated the Si–OH on the structure of regenerated X-zeolite. This analyze show that the regenerated adsorbent has stable structure and desorption process does not effect on the sorbent chemical structure. The FT-IR spectra of the saturated adsorbent, after adsorption of sulfur

Table 2: All of factorial design used for adsorptive desulfurization using AgX-zeolite.

Run Num.	Temp. Des. (°C)	Gas Flow Des. (mL/min)	Time Des. (min)	Temp. Ads. (°C)	Sorbent Metal wt%	Calcination Temp. (°C)	Ads. Yexp. (ppm)	Des. Yexp. (ppm)
1	225	0.5	90	120	5.25	500	52	141
2	300	2	90	120	5.25	200	131	60
3	150	3.5	60	75	5.25	350	51	125
4	225	2	60	75	0.5	500	108	73
5	300	2	30	120	0.5	350	113	63
6	225	2	60	75	5.25	350	52	72
7	300	3.5	60	75	5.25	350	70	58
8	225	3.5	30	75	10	200	117	91
9	150	0.5	60	30	0.5	350	112	230
10	225	3.5	90	30	5.25	500	74	61
11	225	2	60	75	5.25	350	54	76
12	225	2	60	30	10	350	101	70
13	300	0.5	60	75	10	500	93	65
14	150	2	30	120	10	350	62	209
15	225	0.5	30	75	5.25	350	56	151
16	225	2	30	30	5.25	200	116	68
17	150	2	90	75	0.5	200	200	169

Table 3: Physical and Chemical properties of fresh and regenerated AgX –zeolites.

Sample	Metal ion	Metal- impregnated wt%	S_{BET} (m^2/g)	V_t (cm^3/g)	L (nm)
AgX-zeolite (Regenerated)	Ag	5.53	211.03	0.1786	3.1018
AgX-zeolite (Fresh)	Ag	5.53	230..16	0.1826	3.1729

compounds (thiophene) (ax), The band at 2923 and 2862 cm^{-1} can be observed in (axt) which is assigned to the C−H stretching vibration of saturated CH_2 and CH_3, indicating some of the adsorbed sulfur compounds (thiophene) can undergo the opening of its sulfur compounds (thiophenic) ring in adsorption processes, the change on the molecular structure has taken place the performance of fresh and regenerated sorbents are depending on surface chemistry in the adsorption/desorption process and pore structure is very suitable for study in this field. The nitrogen adsorption/ desorption isotherms of improved X-zeolite at 77 K are shown in Table 3 notices the pore size distributions for fresh and regenerated adsorbents. Pore distribution was much centered and uniform about 2 nm. The total pore volume and the BET surface area of fresh and regenerated adsorbents are in Table 3. Total pore volume and the BET surface in fresh and regenerated adsorbents don't have much difference and those result means that regeneration process does not have much effect on adsorbent structure. Also metal percent is completely constant in fresh and regenerated adsorbents. Adsorption and desorption processes do not decrease impregnated metal percent fresh and regenerated adsorbents. However, the pore size of fresh improved zeolite is similar to that of regenerated adsorbent (Table 3).

The particle/crystal morphology of the fresh and regenerated adsorbents was studied by TEM in Fig. 2(a), Fig. 2(b). TEM images of fresh and regenerated adsorbents, based on 13X-zeolite, noticed well formed crystallites /particles of cubic shape and nano size with

Table 4: ANOVA for response surface quadratic model (Y).

Source	Sum of squares		d.f.		Mean square		*F*-Value		*p* > *F*		Remark	
Process	Ads.	Des.	Ads.	Des.	Ads.	Des.	Ads.	Des.	Ads.	Des.	Ads.	Des.
Model	24440.02	49424.42	9	9	2715.56	5491.6	36.11	190.26	< 0.0001	< 0.0001	Significant	Significant
A	253.13	29646.12	1	1	253.13	29646.12	3.37	1027.09	0.1092	< 0.0001		
B	3200	7938	1	1	3200	7938	42.55	275.01	0.0003	< 0.0001		
C	7021.13	861.13	1	1	7021.13	861.13	93.36	29.83	< 0.0001	0.0009		
AB	400	2401	1	1	400	2401	5.32	83.18	0.0545	< 0.0001		
AC	342.25	342.25	1	1	342.25	342.25	4.55	11.86	0.0703	0.0108		
BC	1156	100	1	1	1156	100	15.37	3.46	0.0057	0.1050		
A^2	19.92	4039.79	1	1	19.92	4039.79	0.26	139.96	0.6227	< 0.0001		
B^2	6216.76	1177.79	1	1	6216.76	1177.79	82.66	40.80	< 0.0001	0.0004		
C^2	5062.55	2126.84	1	1	5062.55	2126.84	67.31	*73.68*	< 0.0001	< 0.0001		
Residual	526.45	202.05	7	7	75.21	28.86						
Lack of fit	285.25	165.25	3	3	95.08	55.08	1.58	5.99		0.0583	Not Significant	Not Significant
Pure error	241.2	36.8	4	4	60.3	*9.20*						
Cor. total	24966.47	49626.47	18	16								

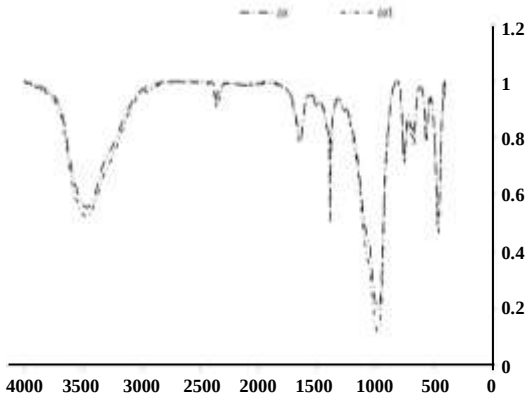

Fig. 3: FT-IR spectra of nano Ag-13X(ax)and adsorbed thiophene over nano Ag-13X(axt).

flat surfaces and sharp edges. Crystallites and particle size of regenerated adsorbents are constant after desorption.

Parameters effect on adsorption/desorption Efficiency

To predict the optimal conditions for sulfur compounds (thiophene) adsorption onto the improved zeolite and sulfur compounds desorption from regenerated adsorbent, axial points were added to the full factorial design with a central point the fit summary of the output indicates that the quadratic model is statistically highly significant for the present adsorption-desorption system. ANOVA is a statistical technique that subdivides the total variation in a set of data into component parts associated with specific sources of variation for the purpose of testing hypotheses on the parameters of the model. The statistical significance of the ratio of mean square variation due to regression and mean square residual error was tested using the analysis of variance (ANOVA). The ANOVA analysis (Table 4) indicates that the most important individual effect for fresh and regenerated nano AgX-zeolite adsorption/desorption of sulfur compounds (thiophene) was the followed by the adsorption temperature (P = 0.1092), metal percent (P = 0.0003), calcination temperature (P < 0.0001), desorption temperature (P < 0.0001), desorption gas flow (P < 0.0001) and desorption time (P < 0.0009). Study the combined effect of these factors; experiments were performed for different combinations of the physical parameters using statistically designed experiments. The results of the Y (response) of adsorption/desorption of sulfur compounds (thiophene) onto nano AgX-zeolite were measured according to the measured responses and design matrix are listed in Table 2.

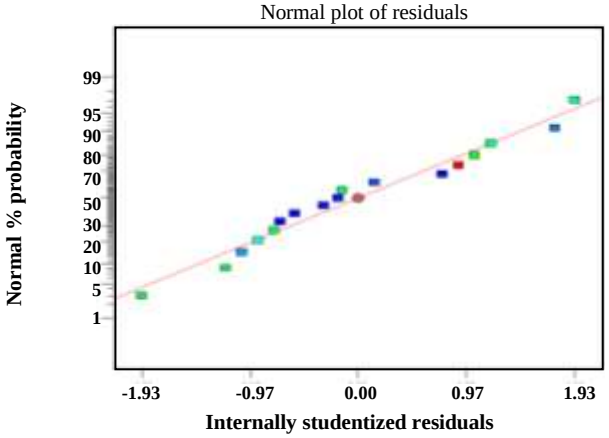

Fig. 4: Scatter diagram of normal % probability versus internally studentized residual for adsorption of thiophene on zeolite.

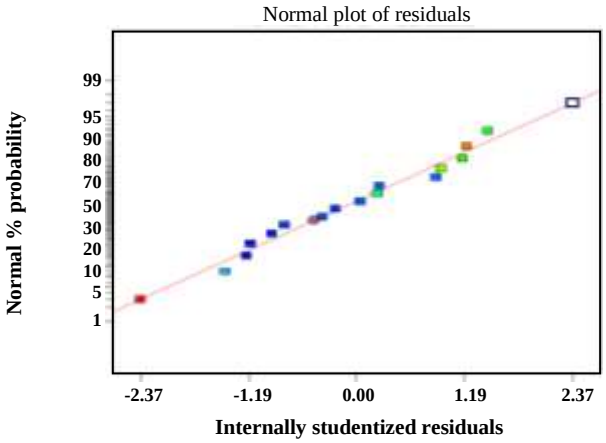

Fig. 5: Scatter diagram of normal % probability versus internally studentized residual for regenerated process.

The actual and the predicted sulfur compounds (thiophene) removal and desorption of sulfur compounds (thiophene) values are given in Figs. 4, 5. The data points on this plot lie reasonably close to a straight line and the model adequately explains the experimental range studied. The actual sulfur compounds (thiophene) removal value and regeneration adsorbent value are the measured result for a specific runs and the predicted values are evaluated from the independent variables in the BBD models.

Results demonstrated that the sulfur compounds (thiophene) desorption from nano AgX-zeolite adsorbent increases with optimal desorption temperature, gas flow rate and regeneration time and adsorption capasity was raised with increasing calcination temperature. The sulfur compounds (thiophene) adsorption raised with the surface area of X-zeolite having more adsorptive sites. The metal percent on adsorbent plays an important role irrespective of the other experimental parameters with increasing M-S (Metal-Sulfur) interactions and adsorptive sites. In the other hands desorption temperature have the vital role in desorption process due to increasing sulfur compounds (thiophene) desorption as SO_2 molecules. Each contour plot represents a number of combinations of two test variables with the other variable maintained at different levels. A way to predict the relationships between factors and interactions and responses is to analyze the contour plots. The contours of the response surface were plotted versus the levels of desorption temperature-desorption time, desorption temperature-desorption gas flow rate, desorption time-desorption gas flow for desorption process (Fig. 6(a)), adsorption temperature-metal percent, calcination temperature-adsorption temperature and calcination temperature-metal percent for adsorption process as shown in, Fig. 6(b). In adsorption the most important dual effect was the interaction between calcination temperature and metal percent ($P < 0.0057$) and in desorption between temperature and gas flow($P < 0.0001$). The second most important effect in adsorption was the interaction between adsorption temperature and metal percent ($P = 0.0545$) and in desorption between desorption temperature and desorption time ($P < 0.0108$). The least interaction in adsorption process was between adsorption temperature and calcination temperature ($P = 0.0703$) and in desorption between desorption time and desorption gas flow ($P < 0.1050$). A high value of the adjusted determination coefficient (R^2 Adj = 0.9789) was recorded for adsorption process and that (R^2 Adj = 0.9959) was recorded for desorption process. These results denoted that 97.9% of the total variation on sulfur compounds (thiophene) adsorption data and 99.6% of the total variation on sulfur compounds desorption data can be described by the selected model. The adequate precision ratio of 22.158 for the quadratic model indicates an appropriated signal to noise ratio for adsorption process and this item for desorption process is 44.836. Since the adequate precision ratio and adjusted determination coefficient exceeded 4 and 70% respectively for adsorption process and these items for desorption process exceeded 4 and 95% respectively, the quadratic model can be used to find the optimal conditions and to explore the design space of

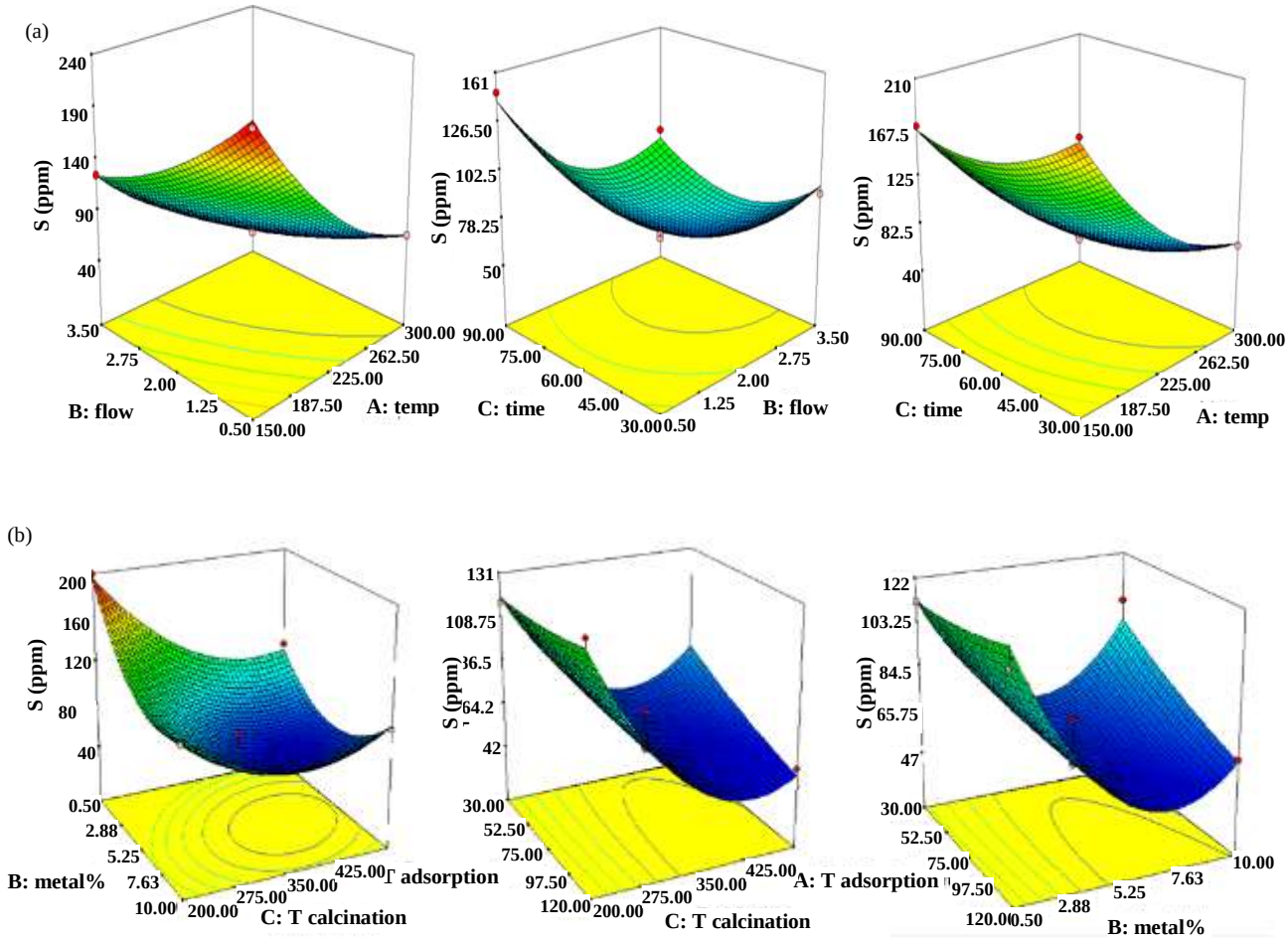

Fig. 6: Response surface graph in three dimensions (a) regeneration process vs. gas flow, process time and desorption temperature for regeneration system, (b) sulfur removal vs. metal percent, calcination temperature and adsorption temperature for thiophene –zeolite adsorption system.

adsorption and desorption processes. Metal percent and calcination temperature had the most significant effects on sulfur compounds (thiophene) adsorption with metal percent 5.53 wt% at calcination temperature of 436 °C also desorption temperature and desorption gas flow had the most significant effects on sulfur compounds (thiophene) desorption at desorption temperature 234 °C with desorption gas flow 2.4 mL/min. The model predicted adsorption efficiency of sulfur compounds (thiophene) is close to 50 ppm onto improved nano X-zeolite and onto regenerated nano AgX-zeolite is 52 ppm, because the level of metal percent, adsorption temperature, calcination temperature for adsorption and desorption temperature, desorption gas flow and desorption time were set on maximum desirability. The importance of each goal was changed in relation to the other goals.

By seeking from 17 starting points (each process) in the response surface changes, the best local maximum was found (Fig. 6(a), Fig. 6(b)). The results are closely related to the data obtained from optimization analysis using desirability functions, indicating BBD (Box–Behnken design) in corporate with desirability functions could be effectively used to optimize the adsorption and desorption parameters for the removal of sulfur compounds (thiophene) and adsorbent regeneration by used. (Table 5).

The application of the response surface methodology based on the estimates of the parameters indicated an empirical relationship between the response and the input variables expressed by the following fitted equation:

$$Y_{des} = 71.8 - 60.87A - 31.5B - 10.38C - 24.5AB + 9.25AC - 5BC + 30.98A^2 + 16.73B^2 + 22.47C^2$$

Table 5: The best operating condition for produce fresh adsorbent and regeneration process.

Process	Adsorption Temp (°C)	Desorption Temp (°C)	Adsorbent Metal wt%	Desorption Gas flow (mL/min)	Adsorbent Calcination Temp. (°C)	Desorption Time (min)
Range and Level	83	---	5.53	---	436	---
	---	234	---	2.4	---	72

Y_{ads} =56.4 -5.62A -20B-29.63C-10AB-9.25AC+17BC+ $2.18A^2$+$38.4B^2$+$34.68C^2$

CONCLUSIONS

In this work, sulfur compounds adsorption onto nano AgX-zeolites and regeneration them was investigated. Experiments were carried out as a function of desorption temperature, desorption gas flow rate, desorption time and adsorption temperature, calcination temperature, metal percentage for desorption and adsorption processes respectively. RSM (Response surface methodology) was used by Box–Behnken design method for role investigation of adsorption and regeneration process factors on sulfur compounds. It was found out that a R^2 (coefficient of determination) value was found to be 0.9959 with second-order polynomial model and F-value of 5.99 for regeneration for desorption process and R_2 (coefficient of determination) value was found to be 0.9789 with second-order polynomial model and F-value of 1.58 based on maximum adsorption amount of sulfur compounds. This investigation demonstrated that the Box–Behnken method is suitable to optimize the experiments for sulfur compounds adsorption and regeneration nano improved adsorbent. The contours show that the increasing metal percentage decreases sulfur compounds adsorption and by increasing calcination temperature sulfur compounds adsorption increases. Also by increasing gas flow rate, desorption time and desorption temperature increase regeneration efficiency.

Acknowledgement

The authors wish to thank Technology Development Division, Research Institute of Petroleum Industry Refining, Tehran, Iran and Chemistry departments, Amirkabir University of Technology, Tehran, Iran for their assistance.

Received: Feb. 2, 2015 ; Accepted : Jul. 18, 2017

REFERENCES

[1] Salazar J.M., Lectez S., Gauvin C., Macaud M., Bellat J.P., Weber G., Bezverkhyy I., Simon J.M., Adsorption of Hydrogen Isotopes in the Zeolite NaX: Experiments and Simulations, *Int. J. of Hydrogen Energy*, **42**(18): 13099–13110(2017).

[2] Chen H., Wang W., Ding J., Wei X., Lu J., CO_2 Adsorption Capacity of FAU Zeolites in Presence of H_2O: A Monte Carlo Simulation Study, *Energy Procedia*, **105**: 4370-4376(2017).

[3] Girimonte R., Formisani B., Testa F., Adsorption of CO_2 on a Confined Fluidized bed of Pelletized 13X Zeolite, *Powder Technology*, **311**(15): 9-17 (2017).

[4] Nakrani D., Belani M., Bajaj H.C., Somani R. S., Singh P.S., Concentrated Colloidal Solution System for Preparation of Uniform Zeolite-Y Nanocrystals and Their Gas Adsorption Properties, *Microporous and Mesoporous Materials*, **241 (15):** 274-284(2017).

[5] Goleij M., Fakhraee H., Response Surface Methodology Optimization of Cobalt (II) and Lead(II) Removal from Aqueous Solution Using MWCNT-Fe_3O4 Nanocomposite, *Iran. J. Chem. Chem. Eng. (IJCCE)*, Article in Press (2017).

[6] Cai J., Li L., Lv X., Yang Ch., and Zhao X., Large Surface Area Ordered Porous Carbons via Nanocasting Zeolite 10X and High Performance for Hydrogen Storage Application, *ACS Applied Materials & Interfaces*, **6**:167-175(2014).

[7] Izadyar S.and Fatemi Sh., Fabrication of X Zeolite Based Modified Nano TiO_2 Photocatalytic Paper for Removal of VOC Pollutants under Visible Light, *Ind. Eng. Chem. Res*., **52**: 10961−10968(2013).

[8] Seyed Hosseini N., Fatemi Sh., Experimental Study and Adsorption Modeling of COD Reduction by Activated Carbon for Wastewater Treatment of Oil Refinery, *Iran. J. Chem. Chem. Eng. (IJCCE)*, **32**: 81–89(2013).

[9] Wan Ch., Ding Sh., Zhang Ch., Tan X., Zou W., Liu X., Yang X., Simultaneous Recovery of Nitrogen and Phosphorus from Sludge Fermentation Liquid by Zeolite Adsorption: Mechanism and Application, *Separation and Purification Technology*, **180 (8)**: 1-12 (2017).

[10] Domínguez-Monterroza A.R., Trujillo C.A., Fractal Analysis at Mesopore Scale of Modified USY Zeolites by Nitrogen Adsorption: A Classical Thermodynamic Approach, *Microporous and Mesoporous Materials*, **237**: 260-267(2017).

[11] Kumar D.R., Chandra Srivastava V., Studies on Adsorptive Desulfurization by Activated Carbon, *Clean – Soil, Air, Water*, **40** (5): 545–550(2012).

[12] Taghizadeh M., Asgharinezhad A.A., Pooladi M., Barzin M., Abbaszadeh A., Tadjarodi A., A Novel Magnetic Metal Organic Framework Nanocomposite for Extraction and Preconcentration of Heavy Metal Ions and Its Optimization Via Experimental Design Methodology, *Microchim Acta*, **180**: 1073–1084 (2013).

[13] Zandevakili S, Ranjbar M, Ehteshamzadeh M., Synthesis of Lithium Ion Sieve Nanoparticles and Optimizing Uptake Capacity by Taguchi Method, *Iran. J. Chem. Chem. Eng. (IJCCE)*, **33**: 15-24 (2014).

[14] Afzal A, Muhammad Imran A, Muhammad Y, Hayat Kh., Mansoor ul Hassan Sh., A Comparative Study of Alkaline Hydrolysis of Ethyl Acetate Using Design of Experiments, *Iran. J. Chem. Chem. Eng. (IJCCE)*, **32**: 33–47(2013).

[15] Gutiérrez O.Y., Singh S., Schachtl E., Kim J., Kondratieva E., Hein J, Johannes A. Lercher, Effects of the Support on the Performance and Promotion of (Ni) MoS_2 Catalysts for Simultaneous Hydrodenitrogenation and Hydrodesulfurization, *ACS Catal.*, **4**: 1487−1499(2014).

[16] Tang M., Zhou L., Du M., Lyu Zh., Wen X.D., Li X., Ge H., A Novel Reactive Adsorption Desulfurization Ni/MnO adsorbent and its Hydrodesulfurization Ability Compared with Ni/ZnO, *Catalysis Communications*, **61**: 37–40 (2015).

[17] Amer T. Nawaf A, Saba A. Gheni a, Aysar T. Jarullah a, Iqbal M. Mujtaba, Improvement of Fuel Quality by Oxidative Desulfurization: Design of Synthetic Catalyst for the Process, *Fuel Processing Technology*, **138**: 337–343 (2015).

[18] Garc-Gutiérrez J. L., Laredo G.C., Garc-Gutiérrez P., Jiménez-Cruz F., Oxidative Desulfurization of Diesel Using Promising Heterogeneous Tungsten Catalysts and Hydrogen Peroxide, *Fuel*, **138**: 118–125 (2014).

[19] Sun H.Y., Sun L.P., Li F., Zhang L., Adsorption of Benzothiophene From Fuels on Modified NaY Zeolites, *Fuel Processing Technology*, **134**: 284–289 (2015).

[20] Song H., Cui X.H., Song H.L., Gao H.J., and Li F., Characteristic and Adsorption Desulfurization Performance of Ag−Ce Bimetal Ion-Exchanged Y Zeolite, *Ind. Eng. Chem. Res.*, **53**: 14552−14557 (2014).

[21] Bakhtiari Gh., Abdouss M., Bazmi M., Royaee S. J., High Efficiency Desulfurization of Gas Condensate by Adsorption Method on Improved Zeolite, *Afinidad*, **574**:148-155(2016).

[22] Wrabetz S, Yang X, Tzolova-Müller G, Schlgl R, Jentoft F.C., Characterization of Catalysts in Their Active State by Adsorption Microcalorimetry: Experimental Design and Application to Sulfated Zirconia, *Journal of Catalysis*, **269**: 351–358(2010).

[23] Thambidurai M, Muthukumarasamy N, Murugan N, Agilan S, Vasantha S, Balasundaraprabhu R, Development of Mathematical Model for Prediction and Optimization of Particle Size in Nanocrystalline Cds Thin Films Prepared by Sol-Gel Spin-Coating Method, *Metallurgical and Materials Transactions B*, **41B**: 1338–1345 (2010).

[24] Zeng T., Hu X., Ji P., Shang B., Peng Q., Zhang Y., Song R., Promotional Role of $Li_4Ti_5O_{12}$ as Polysulfide Adsorbent and Fast Li^+ Conductor on Electrochemical Performances of Sulfur Cathode, *Journal of Power Sources*, **359**: 250–261 (2017).

[25] Zahedi Abghari S., Shokri S., Baloochi B., Ahmadi Marvast M., Ghanizadeh Sh., Behroozi A., Analysis of Sulfur Removal in Gasoil Hydrodesulfurization Process by Application of Response Surface Methodology, *Korean J. Chem. Eng.*, **28**(1): 93-98 (2011).

[26] Myers R.H., Montgomery D.C., "Response Surface Methodology: Process and Product Optimization Using Designed Experiments", (Wiley Series in Probability and Statistics), Second ed., Wiley, New York, NY, (2002).

[27] Box G.E.P., Wilson K.B., On the Experimental Attainment of Optimum Conditions, *J. Roy. Statist. Soc. Ser*. B 13:1-45 (1951).

[28] Aydın Y.A., Aksoy N.D., Adsorption of Chromium on Chitosan: Optimization, Kinetics and Thermodynamics, *Chem. Eng. J*. **151**: 188–194 (2009).

[29] Chattoraj S., Sadhukhan B., Mondal N.K., Predictability by Box-Behnken Model for Carbaryl Adsorption by Soils of Indian Origin, *J. of Env. Sci. and Health, Part B* **48**: 626-636 (2013).

[30] Dutta S., Optimization of Reactive Black 5 Removal by Adsorption Process Using Box–Behnken Design, *Desalination and Water Treatment*, **1**: 1-8 (2013).

[31] Sayilgan E, Cakmakci O., Treatment of Textile Dyeing Wastewater by Biomass of Lactobacillus: Lactobacillus 12 and Lactobacillus Rhamnosus, *Environ Sci Pollut Res* **20**: 1556-1564 (2013).

[32] Tsao C.C., Comparison Between Response Surface Methodology and Radial Basis Function Network for Core-Centre Drill in Drilling Composite Materials, *Int J Adv. Manuf. Technol*. **37**: 1061-1068 (2008).